Future Changes in extreme precipitation over South Asia and its causes

Mayank Suman & Rajib Maity

Indian Institute of Technology Kharagpur

April 30, 2021

CC BY

Introduction

- Indian Summer Monsoon (ISM) is sensitive to changing climate (Qiu, 2008; Ghosh *et al.*, 2012; Kitoh and Endo, 2016; Krishnan *et al.*, 2016; Mohan and Rajeevan, 2017).
- Little agreement on nature of change.
- Contradicting conclusions might result from differences in:
  - Dataset being studied
  - Selected study regions
  - Characterization of extreme
  - Differences in methodology
- Fine resolution data can help in understanding the dynamics of ISM better (Vinnarasi and Dhanya, 2016).

Analysis of observed Indian Summer Monsoon Rainfall (ISMR)

Literature	Major Findings
Goswami *et al.* (2006), Rajeevan *et al.* (2008)	Extreme and moderate active events in central India have statistically significant positive trend and negative trend respectively
Krishnamurthy *et al.* (2009)	Statistically significant increase in extreme precipitation events post 1980
Singh and Ranade (2010), Singh *et al.* (2014)	Increase in the frequency of dry spell and intensity of wet spell
Rajeevan *et al.* (2010)	No significant trend in extreme precipitation across India
Dash *et al.* (2009)	Dry spell has a positive trend in most parts of India
Vinnarasi and Dhanya (2016)	Significant negative trend in wet spell duration and a positive trend in dry spell

Future status of ISMR

Literature	Major Findings
Ashfaq *et al.* (2009)	Suppression of Indian monsoon.
Ashfaq *et al.* (2009), Loo *et al.* (2015)	A shift in the onset of monsoon along with a change in its duration.
Kitoh and Endo (2016), and Maity *et al.* (2016)	Overall wetter monsoon and an increase in extreme precipitation events.
Donat *et al.* (2016)	South Asia is expected to receive more and Central Asia is expected to receive less precipitation than in the past.

Analysis of observed precipitation

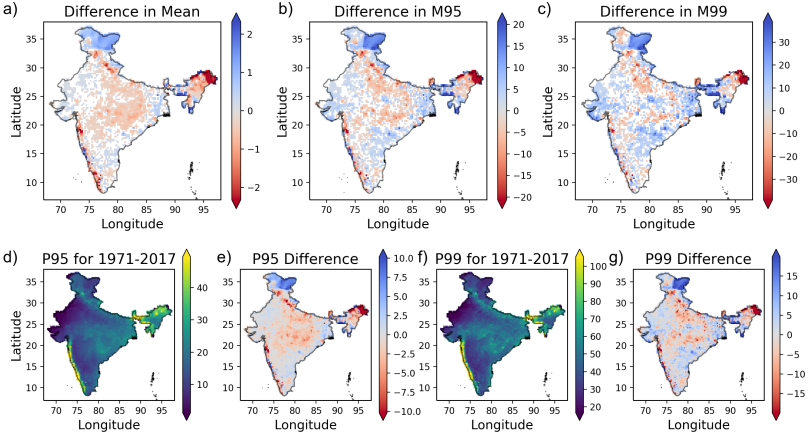

Figure 1: Difference in **a**) mean daily precipitation, **b**) M95 and **c**) M99 (in mm/day) between 1971-2017 and 1930-1970. **d**) P95 (in mm/day) during 1971-2017 and **e**) its difference with respect to 1930-1970. Similar figures (**f**, **g**) for P99. M95 and M99 show mean of the days having precipitation higher or equal to P95 and P99, respectively. Colored patches inside Indian landmass in figures (a-c) are having significant changes. The significance of change in mean precipitation, M95 and M99 is tested using Welch's t-test at 5% level of significance.

Analysis of future precipitation

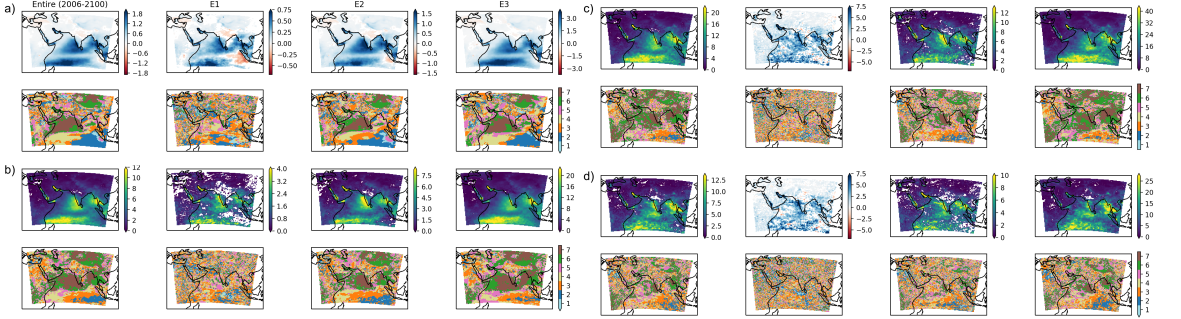

Figure 2: Difference between future and historical (1961-2005) precipitation (mm/day) (**a**, top row) in mean, (**b**, top row) in M95, and (**c**, top row) in M99 for RCP8.5 (**d**, top row) same as (c, top row) but for RCP4.5 for mean Coordinated Regional Downscaling Experiment (CORDEX) ensemble (Table 1). Four columns indicate entire future period (2006-2100) and three epochs: E1 (2006-2035), E2 (2036-2070), and E3 (2071-2100). Areas showing no significant change are shown in white patches. (**a-d**, bottom row): Spatial distribution of number of CORDEX models in agreement.

Analysis of future precipitation

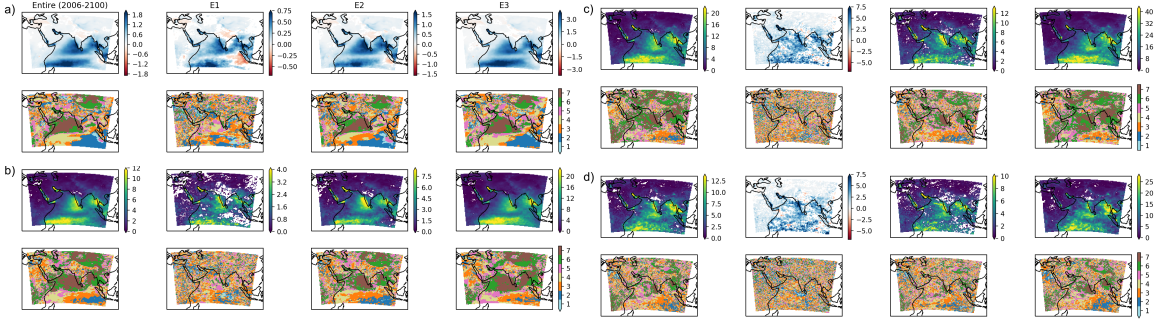

Figure 2: Difference between future and historical (1961-2005) precipitation (mm/day) (**a**, top row) in mean, (**b**, top row) in M95, and (**c**, top row) in M99 for RCP8.5 (**d**, top row) same as (c, top row) but for RCP4.5 for mean CORDEX ensemble (Table 1). Four columns indicate entire future period (2006-2100) and three epochs: E1 (2006-2035), E2 (2036-2070), and E3 (2071-2100). Areas showing no significant change are shown in white patches. (**a-d**, bottom row): Spatial distribution of number of CORDEX models in agreement.

What is reason for these changes?

Possible causes for observed future changes

Major forcings affecting ISM:

- Temperature between Tibetan Plateau and Indian Ocean (Qiu, 2008; Li *et al.*, 2010)
- Warm moist air over India (Rajeevan *et al.*, 2008; Krishnan *et al.*, 2016) insulated by Himalayas (Boos and Kuang, 2010)
- Land use change (Paul *et al.*, 2016)
- Precipitable water content, specific humidity, and Wind Speed at 850mb

Analysis of the air temperature (850mb) and total precipitable water suggests intensified ISM:

- Stronger and frequent positive Indian Ocean Dipole (IOD).
- Higher temperature over Tibetan Plateau and the Himalayas

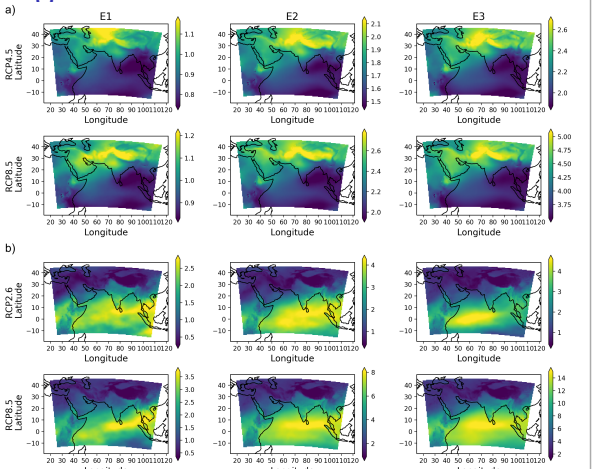

Figure 3: Epochwise change in **a**) air temperature at 850mb (in °C) for mean ensemble CORDEX, and **b**) total precipitable water (in kg/m^2) for REMO2009 Regional Climate Model (RCM) forced by MPI-ESM Global Circulation Model (GCM) when compared to respective historical (1961-2005) mean. There is no region with insignificant change (white patches).

Changes in moisture flux and convergence

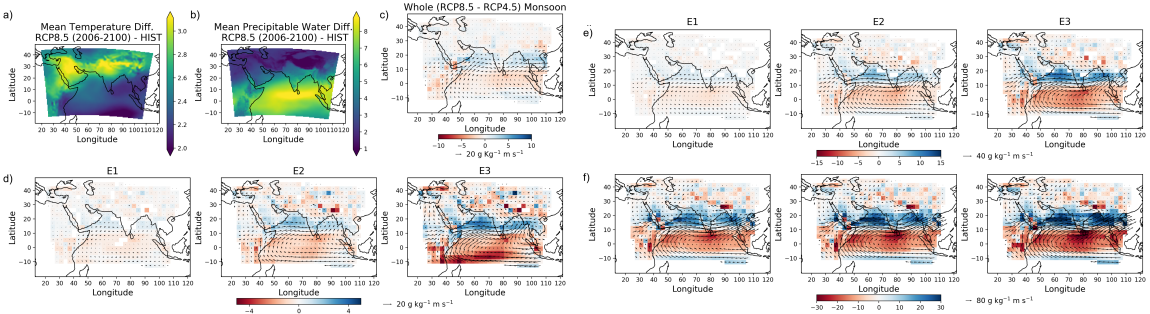

Figure 4: Possible causes of change in precipitation in future. Difference in **a**) mean temperature ($^{\circ}C$) and **b**) mean precipitable water (kg/m^2) at 850mbar between future (2006-2100; RCP8.5) and HIST (1961-2005). **c**) Difference in mean moisture flux ($g\,kg^{-1}ms^{-1}$) and moisture convergence ($g\,kg^{-1}ms^{-1}$ per degree) at 850 mbar between RCP8.5 and RCP4.5 scenarios. Difference in mean condition of moisture flux and convergence between different periods in future (RCP8.5) and HIST by considering **d**) all months **e**) monsoon months. Similarly, difference in mean condition of moisture flux and moisture convergence during extreme events (above P99) for different epochs and mean condition in HIST at region **f**) A2. For figures **(c-f)** the arrow length and direction show magnitude of moisture flux, and direction of moisture flux respectively at 850mbar. Only the regions with significant changes are shown.

Validation of observed future change

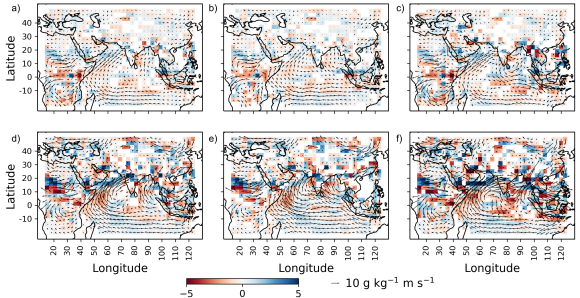

Figure 5: **Change in moisture flux and moisture convergence using ERA-Interim data**. Difference in mean moisture flux (in $g\,kg^{-1}ms^{-1}$) and moisture convergence (in $g\,kg^{-1}ms^{-1}$ per degree) at 850mbar w.r.t. 1979-2000 for the period **a)** 2001 to 2018, **b)** 2001 to 2010, **c)** 2011 to 2018 considering all months. Figure **d-f** is similar to **a-c** but only consider monsoon months. The length and direction of arrows show magnitude and direction of moisture flux respectively at 850mbar. Only the regions with significant changes are shown.

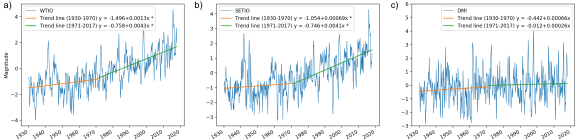

Figure 6: Trend in a) WTIO, b) SETIO, and c) Dipole Mode Index (DMI) for Indian Ocean Dipole pre and post 1970. The trend line equation marked with * are found to be statistically significant at 5% level of significance using Mann-Kendall's Test.

- Analysis of moisture flux and convergence from ERA-Interim indicates that the variables are getting more intensified in Arabian season region during 2011-2018.
- Despite no trend in DMI of IOD, the number of positive IOD event have increased two fold post 1970. Mean DMI have also shown significant increase in the period.

Take Home

- The precipitation extreme events have become more intense in South India (especially east coast) as compared to North India. In future, this contrast will intensify in both magnitude (thus threshold) and frequency.
- The increased temperature over Tibetan Plateau and the Himalayas, intensification of IOD and increased precipitable water will help in intensification of ISM over entire Indian mainland.
- The precipitation extremes are moving south over South Asia. The major reason for this change is eastward shift of moisture flux and high change in moisture convergence over Indian Ocean region (10° to 20°N).
- The moisture contribution from Bay of Bengal is expected to increase for northern India and countries like Myanmar and Thailand etc. However, due to weaker moisture convergence, comparatively less increase in mean daily precipitation over north and central India is expected.
- Overall, the areas expected to have the highest increase in extreme precipitation are Arabian Sea, Southern India, and South-East Asian countries such as Myanmar, Thailand etc.

Further Reading

Suman, Mayank and Rajib Maity (2020). 'Southward shift of precipitation extremes over south Asia: Evidences from CORDEX data'. Scientific Reports 10.1, pp. 1–11.

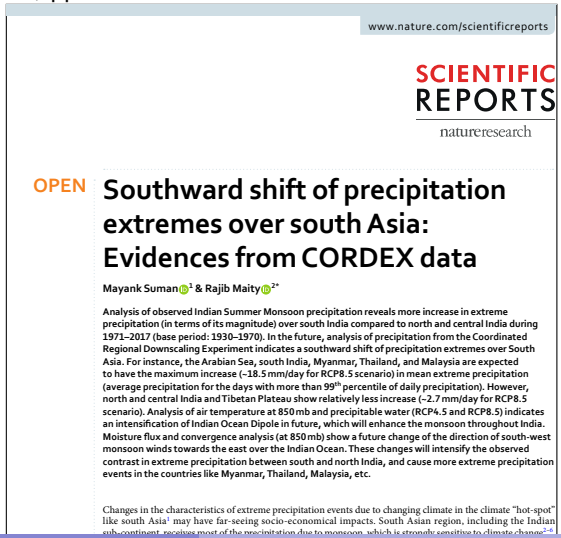

www.nature.com/scientificreports

SCIENTIFIC REPORTS

nature research

OPEN

Southward shift of precipitation extremes over south Asia: Evidences from CORDEX data

Mayank Suman[1] & Rajib Maity[2*]

Analysis of observed Indian Summer Monsoon precipitation reveals more increase in extreme precipitation (in terms of its magnitude) over south India compared to north and central India during 1971–2017 (base period: 1930–1970). In the future, analysis of precipitation from the Coordinated Regional Downscaling Experiment indicates a southward shift of precipitation extremes over South Asia. For instance, the Arabian Sea, south India, Myanmar, Thailand, and Malaysia are expected to have the maximum increase (~18.5 mm/day for RCP8.5 scenario) in mean extreme precipitation (average precipitation for the days with more than 99th percentile of daily precipitation). However, north and central India and Tibetan Plateau show relatively less increase (~2.7 mm/day for RCP8.5 scenario). Analysis of air temperature at 850 mb and precipitable water (RCP4.5 and RCP8.5) indicates an intensification of Indian Ocean Dipole in future, which will enhance the monsoon throughout India. Moisture flux and convergence analysis (at 850 mb) show a future change of the direction of south-west monsoon winds towards the east over the Indian Ocean. These changes will intensify the observed contrast in extreme precipitation between south and north India, and cause more extreme precipitation events in the countries like Myanmar, Thailand, Malaysia, etc.

Changes in the characteristics of extreme precipitation events due to changing climate in the climate "hot-spot" like south Asia[1] may have far-seeing socio-economical impacts. South Asian region, including the Indian sub-continent, receives most of the precipitation due to monsoon, which is strongly sensitive to climate change[2–4]

References

Ashfaq, Moetasim *et al.* (2009). "Suppression of south Asian summer monsoon precipitation in the 21st century". In: *Geophysical Research Letters* 36.1.

Boos, William R and Zhiming Kuang (2010). "Dominant control of the South Asian monsoon by orographic insulation versus plateau heating". In: *Nature* 463.7278, p. 218.

Dash, SK, Makarand A Kulkarni, UC Mohanty, and K Prasad (2009). "Changes in the characteristics of rain events in India". In: *Journal of Geophysical Research: Atmospheres* 114.D10.

Donat, Markus G, Andrew L Lowry, Lisa V Alexander, Paul A O'Gorman, and Nicola Maher (2016). "More extreme precipitation in the world's dry and wet regions". In: *Nature Climate Change* 6.5, p. 508.

Ghosh, Subimal, Debasish Das, Shih-Chieh Kao, and Auroop R Ganguly (2012). "Lack of uniform trends but increasing spatial variability in observed Indian rainfall extremes". In: *Nature Climate Change* 2.2, p. 86.

Goswami, Bhupendra Nath, V Venugopal, D Sengupta, MS Madhusoodanan, and Prince K Xavier (2006). "Increasing trend of extreme rain events over India in a warming environment". In: *Science* 314.5804, pp. 1442–1445.

Kitoh, Akio and Hirokazu Endo (2016). "Changes in precipitation extremes projected by a 20-km mesh global atmospheric model". In: *Weather and climate extremes* 11, pp. 41–52.

Krishnamurthy, Chandra Kiran B, Upmanu Lall, and Hyun-Han Kwon (2009). "Changing frequency and intensity of rainfall extremes over India from 1951 to 2003". In: *Journal of Climate* 22.18, pp. 4737–4746.

References

Krishnan, R *et al.* (2016). "Deciphering the desiccation trend of the South Asian monsoon hydroclimate in a warming world". In: *Climate dynamics* 47.3-4, pp. 1007–1027.

Li, Haibin, Justin Sheffield, and Eric F Wood (2010). "Bias correction of monthly precipitation and temperature fields from Intergovernmental Panel on Climate Change AR4 models using equidistant quantile matching". In: *Journal of Geophysical Research: Atmospheres* 115.D10.

Loo, Yen Yi, Lawal Billa, and Ajit Singh (2015). "Effect of climate change on seasonal monsoon in Asia and its impact on the variability of monsoon rainfall in Southeast Asia". In: *Geoscience Frontiers* 6.6, pp. 817–823.

Maity, Rajib, Ankit Aggarwal, and Kironmala Chanda (2016). "Do CMIP5 models hint at a warmer and wetter India in the 21st century?" In: *Journal of Water and Climate Change* 7.2, pp. 280–295.

Mohan, TS and M Rajeevan (2017). "Past and future trends of hydroclimatic intensity over the Indian monsoon region". In: *Journal of Geophysical Research: Atmospheres* 122.2, pp. 896–909.

Paul, Supantha, Subimal Ghosh, Robert Oglesby, Amey Pathak, Anita Chandrasekharan, and RAAJ Ramsankaran (2016). "Weakening of Indian summer monsoon rainfall due to changes in land use land cover". In: *Scientific Reports* 6, p. 32177.

Qiu, Jane (2008). "China: the third pole". In: *Nature News* 454.7203, pp. 393–396.

Rajeevan, M, J Bhate, and Ashok K Jaswal (2008). "Analysis of variability and trends of extreme rainfall events over India using 104 years of gridded daily rainfall data". In: *Geophysical Research Letters* 35.18.

References

Rajeevan, M, Sulochana Gadgil, and Jyoti Bhate (2010). "Active and break spells of the Indian summer monsoon". In: *Journal of earth system science* 119.3, pp. 229–247.

Singh, Deepti, Michael Tsiang, Bala Rajaratnam, and Noah S Diffenbaugh (2014). "Observed changes in extreme wet and dry spells during the South Asian summer monsoon season". In: *Nature Climate Change* 4.6, p. 456.

Singh, Nityanand and Ashwini Ranade (2010). "The wet and dry spells across India during 1951–2007". In: *Journal of Hydrometeorology* 11.1, pp. 26–45.

Vinnarasi, R and CT Dhanya (2016). "Changing characteristics of extreme wet and dry spells of Indian monsoon rainfall". In: *Journal of Geophysical Research: Atmospheres* 121.5, pp. 2146–2160.

Thank You

Additional Slides

Analysis of future daily precipitation

Table 1: Details of different CORDEX simulation outputs used

S.No.	RCM Used	GCM Forcing	Spatial Resolution	Institute
1	REMO2009 *	MPI-ESM-LR	0.5° lat × 0.5° lon	MPI-CSC^{+}
2	RegCM4	CCCma-CanESM2	50 km by 50 km	IITM^{++}
3	RegCM4	CNRM-CM5	50 km by 50 km	IITM
4	RegCM4	CSIRO-Mk3.6.0	50 km by 50 km	IITM
5	RegCM4	IPSL-CM5A-LR	50 km by 50 km	IITM
6	RegCM4	MPI-ESM-MR	50 km by 50 km	IITM
7	RegCM4	GFDL-ESM2M	50 km by 50 km	IITM

* Scenario RCP2.6 (additionally) available. All models have RCP4.5 and RCP8.5 scenarios. $^{+}$ Climate Service Center, Max Planck Institute for Meteorology. $^{++}$ Indian Institute of Tropical Meteorology

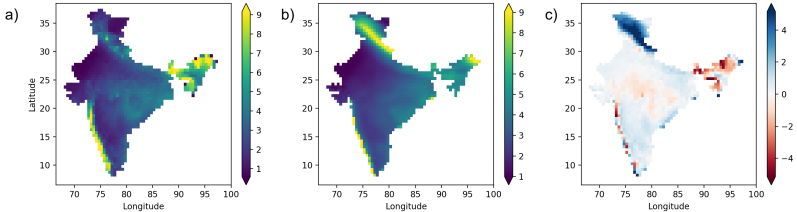

Figure 7: Bias in ensemble mean CORDEX for historical period (1961-2005). **a)** Mean daily precipitation (mm/day) for observed ISMR, **b)** Mean daily precipitation (mm/day) for ensemble mean CORDEX precipitation. **c)** The corresponding bias in mean precipitation

Mann-Kendall Trend Analysis

The Mann-Kendall statistic (S) for the test is given by:

$$S = \sum_{i=1}^{n-1} \sum_{j=i+1}^{n} sign(x_j - x_i) \tag{1}$$

where $sign(a) = {}^{|a|}/_{a}$ for $a \neq 0$ and 0 for $a = 0$. The variance of the Mann-Kendall statistics is given by:

$$V_S = \frac{1}{18}\left[n(n-1)(2n+5) - \sum_{k=1}^{g} f_k(f_k-1)(2f_k+5)\right] \tag{2}$$

where n is the data length, g is the total number of tied groups, and f_k is number of samples in k^{th} tied group. The test statistics (z) follow standard normal distribution and is given by:

$$z = \frac{S - sign(S)}{\sqrt{V_S}} \tag{3}$$

Null hypothesis of no trend can be rejected at $\alpha\%$ level of significance if $|z| > Z_{\alpha/2}$ (for two sided test).

Welch's t test

The test statistic (t) is given by:

$$t = \frac{\overline{X}_1 - \overline{X}_2}{\sqrt{S_1^2/N_1 + S_2^2/N_2}} \tag{4}$$

where X_i, S_i and N_i are mean, standard deviation, and sample size of ith precipitation series respectively.

The t test statistics approximately follows Student's t distribution with ν degrees of freedom. The value of ν is estimated as:

$$\nu = \frac{\left(S_1^2/N_1 + S_2^2/N_2\right)^2}{S_1^4/N_1^2\nu_1 + S_2^4/N_2^2\nu_2} \tag{5}$$

where $\nu_i = N_i - 1$ is degree of freedom associated with i^{th} variance estimate (S_i^2).

For two sided test at $\alpha\%$ level of significance, the null hypothesis of equal mean can be rejected if $t \geq t_{\alpha/2}(\nu)$.

Student's t test

The test statistic (t) is given by:

$$t = \frac{\overline{X}_1 - \overline{X}_2}{S_p \sqrt{1/N_1 + 1/N_2}} \qquad S_p = \sqrt{\frac{S_1^2(N_1 - 1) + S_2^2(N_2 - 1)}{N_1 + N_2 - 2}} \tag{6}$$

where X_i, S_i and N_i are mean, standard deviation, and sample size of ith precipitation series respectively. S_p is pooled standard deviation.

The t test statistics follows Student's t distribution with $N_1 + N_2 - 2$ degrees of freedom. Hence, for two sided test at $\alpha\%$ level of significance, the null hypothesis of equal mean can be rejected if $t \geq t_{\alpha/2}(N_1 + N_2 - 2)$.

Why Welch's t-test is used?

Welch's t-test is more robust than Student's t test, especially for large sample sizes. Student's t- test is not effective when two population are expected to have unequal variances. However, Welch's t-test do not suffer from such problems.

Hotelling's t^2 test

The test statistics of Hotelling's t^2-test is given by:

$$t^2 = \frac{N_1 N_2}{N_1 + N_2} \left(\overline{X}_1 - \overline{X}_2\right)^T \hat{\Sigma} \left(\overline{X}_1 - \overline{X}_2\right) \tag{7}$$

where $\overline{X}_i$ represent vector of mean of variable X in orthogonal directions for i^{th} period, hence, $\overline{X}_i = \left[\overline{X}_{ix},\ \overline{X}_{iy}\right]^T$. N_i is size of sample for i^{th} period. $\hat{\Sigma}$ shows the pooled covariance matrix given by:

$$\hat{\Sigma} = \frac{(N_1 - 1)\Sigma_1 + (N_2 - 1)\Sigma_2}{N_1 + N_2 - 2} \tag{8}$$

where Σ_i represents covariance matrix for components of X_i.

The null hypothesis of mean of components being equal across different populations at $\alpha\%$ level of significance can be rejected, if $\frac{N_1+N_2-p-1}{(N_1+N_2-2)p} t^2 \geq F_{\alpha/2}(p, N_1 + N_2 - p - 1)$ (for two sided test), where p is number to vector components (*i.e.*, 2 in this case).

Moisture Flux and convergence

- Moisture Flux represents the net moisture movement at a particular height and is given by

$$\vec{Q} = q\vec{V} \tag{9}$$

where $\vec{Q}$ is moisture flux, q is specific humidity,and $\vec{V}$ is wind velocity (with components u and v).

- Moisture Flux Convergence or Moisture Convergence: Measure of degree to which moist air is converging into an area.

$$Q_c = -\nabla \cdot \vec{Q} = -\frac{\partial Q_x}{\partial x} - \frac{\partial Q_y}{\partial y} = -u\frac{\partial q}{\partial x} - v\frac{\partial q}{\partial y} - q\left(\frac{\partial u}{\partial x} + \frac{\partial v}{\partial y}\right) \tag{10}$$

where Q_x and Q_y are component of $\vec{Q}$ in x and y direction, respectively.

Areas of persistent moisture convergence are favored regions for thunderstorm development, if other factors (e.g., instability) are favorable.